이학석사 학위논문

커드란 투여 SKG 마우스에서 흡연이 자가면역관절염에 미치는 영향.

Influence of cigarette smoke on autoimmune arthritis in curdlan administered SKG mice.

울산대학교 대학원

의과학과

이재현

커드란 투여
SKG 마우스에서 흡연이
자가면역관절염에 미치는 영향.

지도교수 김용길

이 논문을 이학석사학위 논문으로 제출함

2022 년 8 월

울 산 대 학 교 대 학 원

의 과 학 과

이 재 현

이재현의 이학석사학위 논문을 인준함

심사위원장 홍 석 찬 (인)

심사위원 김 용 길 (인)

심사위원 장 은 주 (인)

울 산 대 학 교 대 학 원

2022 년 8 월

Abstract

Background: The cholinergic anti-inflammatory pathway involves the interaction between the autonomic nervous system and the immune system. For example, the acetylcholine receptor alpha7 nicotinic acetylcholine receptor (α7nAChR) is expressed in both synoviocytes and various immune cells. In the anti-inflammatory pathway, α7nAChR downregulates proinflammatory cytokines. Growing evidence suggests that nicotine and cotinine, a major metabolite of nicotine, may have anti-inflammatory properties in autoimmune arthritis by activating α7nAChR on immune cells, and synovial expression of α7nAChR was increased in patients with active rheumatoid arthritis. However, little is known about the synovial expression of α7nAChR and the effect of smoking in spondyloarthropathy (SpA). Therefore, we evaluated the synovial expression of α7nAChR and the effect of cigarette smoke on peripheral arthritis and spinal ankylosis in curdlan-administered SKG mice, a murine model of SpA.

Purpose: We evaluated the synovial expression of α7nAChR and effect of smoking on peripheral arthritis and spinal ankylosis in curdlan-administered SKG mice, murine models of spondyloarthropathy.

Methods: Curdlan was injected into the mice twice at a 2-week interval. The curdlan-administered SKG mice were placed into two groups; one group that inhaled cigarette smoke (from four cigarettes for 15 min three times with a 10 min rest repeat) 5 days a week for 20 weeks starting with the first curdlan injection and one group that did not inhale smoke. Serum cotinine levels were measured at 16

weeks post-curdlan injection. Clinical scores for peripheral arthritis were evaluated every week after curdlan injection, and a histological evaluation was performed at 23 weeks post-curdlan injection. To evaluate osteoblastic activity in the spine, imaging was performed using the fluorescent in vivo bisphosphonate agent OsteoSense® 680 EX at 21 weeks post-curdlan injection. The auto-reactive T cell population in splenocytes was examined using immunohistochemical staining and flow cytometry.

Results: At 23 weeks post-curdlan injection, α7nAChR$^+$ and α7nAChR$^+$ T_H17 cells were increased in the synovia of curdlan-administered SKG mice. Metabolomic analysis at 16 weeks post-curdlan injection showed that cotinine was increased in smoke-exposed mice. Peripheral arthritis scores were better in smoke-exposed curdlan-administered SKG mice than in unexposed mice. Similarly, the histologic examination scores for synovial inflammation were also lower in smoke-exposed curdlan-administered SKG mice than in unexposed mice. However, osteoblastic activities in the spine, as measured by the fluorescence of hydroxyapatite, did not differ between the groups. In the flow cytometry analysis, the T_H17 and T_{reg} populations did not differ between the groups. However, the IL-17A$^+$ T_{reg} population was decreased in smoke-exposed model mice. The percentages of IL-17A$^+$, FOXP3$^+$, and IL-17A$^+$FOXP3$^+$ cells were decreased in the synovia of smoke-expose curdlan-administered SKG mice compared to that in unexposed model mice.

Conclusion: Our results suggest that cigarette smoke might have an anti-arthritogenic effect by increasing cotinine levels in curdlan-administered SKG mice, which have abundant α7nAChR$^+$ cells in the synovia.

Keywords: Spondyloarthropathy, SKG mice, T cells, cigarette, cotinine

CONTENTS

INTRODUCTION

Spondyloarthropathy (SpA) is an inflammatory rheumatic disease that shows manifestations such as chronic back pain, arthritis, enthesitis and dactylitis [1]. Although there is much to be learned about the disease, interactions between genetic factors, especially human leukocyte antigen-B27, and various stresses induce the production of pro-inflammatory cytokines and risk factors [2]. Interleukin-17 (IL-17) plays a pro-inflammatory role in SpA, and many studies have been conducted on IL-17-producing cells, especially T helper 17 (TH,17) cells [3]. Recent findings indicate that the increase in the number of T_H17 cells in patients with ankylosing spondylitis (AS) may be due not only to the differentiation of naive T cells but also to a reduction in the plasticity of T_H17 cells [4]. Forkhead box P3 (FOXP3) is essential for the suppressive function of regulatory T (T_{reg}) cells, which are immune-suppressive cells that maintain immune homeostasis. In inflammatory arthritis, $CD25^{lo}FOXP3^{+}CD4^{+}$ T cells can lose FOXP3 expression and convert to T_H17 cells [5, 6]. The synovium of patients with rheumatoid arthritis (RA) and arthritic DBA mice contained increased numbers of $IL\text{-}17A^{+}FOXP3^{+}$ T cells, which probably represent an intermediate stage in the transition of $FOXP3^{+}$ T cells to T_H17 cells [5, 6].

Alpha7 nicotinic acetylcholine receptor (α7nAChR) plays an important role in the cholinergic anti-inflammatory pathway, not only by inhibiting the release of cytokines but also by regulating the activity of immune cells. It is also involved in autoimmune arthritis [7]. α7nAChR is expressed in the synovia of patients with

RA, and α7nAChR expression was observed in cultured RA fibroblast-like synoviocytes. Treatment with agonists of α7nAChR reduced the levels of the pro-inflammatory cytokines IL-6 and IL-8 [8], and α7nAChR-specific agonists reduced the clinical arthritis score and histological score in a model of collagen-induced arthritis (CIA) [9]. α7nAChR is expressed in a variety of immune cells, including dendritic cells, T and B lymphocytes, monocytes, and macrophages [7]. It has been reported that over 90% of human T_H17 cells express α7nAChR, and IL-17 expression decreases when α7nAChR is activated by nicotine [10]. T_{regs} also express α7nAChR, and signaling through α7nAChR regulates their immunosuppressive effect by reducing inflammatory cytokines and increasing FOXP3 [11]. Macrophages express α7nAChR, and receptor activation by nicotine increased their anti-inflammatory phenotype and inhibited the inflammatory phenotype in the decidua of a mouse model of preeclampsia [12].

Nicotine, a major component of cigarettes, has been reported to have an immunomodulatory effect in inflammatory diseases [13]. Although nicotine often has harmful effects on immune-mediated diseases, several studies have shown a beneficial effect in autoimmune arthritis [13]; nicotine reduced clinical arthritis scores and IL-17A levels in CIA mice by activating α7nAChR on T_H17 cells [14], and administration of nicotine reduced both clinical arthritis scores and macrophage accumulation in the synovium [15]. Nicotine is converted to cotinine [16, 17], which has anti-inflammatory effects on human monocytes by reducing the production of pro-inflammatory cytokines, such as tumor necrosis factor-α and IL-

1β, through α7nAChR [18]. Cotinine is being studied as a potential treatment for Parkinson's disease, which is characterized by neuroinflammation [19]. However, its effects in arthritis are largely unknown

CIA mice, a widely used animal model of autoimmune arthritis, do not show the characteristics of SpA; self-resolution occurs around 60 days after inoculation, and IL-17A has a major impact on arthritis, but even without IL-17A, arthritis occurs in this model [20]. In contrast, SKG mice have the characteristics of human SpA, including peripheral arthritis, enthesitis, and inflammatory bowel disease [21]. These mice have a point mutation in the gene encoding ZAP-70 (in the SH2 domain), a key signal transduction molecule in T cells [22]. They have the potential to develop peripheral arthritis in the early stage and spinal ankylosis in the late stage via autoreactive T cells partially through IL-17A/IL-22 and IL-23 signaling, especially when exposed to a beta-glucan such as curdlan [23, 24].

To the best of our knowledge, there are no published studies on the relationship between α7nAChR and SpA. Therefore, we aimed to evaluate how activation of α7nAChR affects an animal model of autoimmune arthritis and the effects of cotinine induced by cigarette smoke exposure on peripheral arthritis and spinal ankylosis in curdlan-administered SKG mice.

METHODS

Immunofluorescent staining

Multiplexed immunofluorescent staining of mouse hind tissue was performed using the Opal method (Perkin Elmer, Waltham, MA, USA). Primary antibodies were sequentially applied to a single slide as described below. The slides were deparaffinized with xylene and rehydrated using ethanol. For antigen retrieval, the slides were heated in a citrate buffer (pH 6.0) using a microwave. Slides were first incubated with primary rabbit antibodies to α7nAChR (ab216485, 1:500; Abcam, Cambridge, MA, USA) in a humidified chamber at 37 °C for 1 h and then with horseradish peroxidase (HRP) Mouse (Ms) + Rabbit (Rb). α7nAChR was visualized using fluorescein Opal 520 (1:100). Then, the slide was placed in citrate buffer (pH 6.0) and heated using a microwave. After the slides cooled, they were incubated with primary rabbit antibodies to FOXP3 (ab215206, 1:1000; Abcam) overnight (~14 h) in a humidified chamber at 4 °C, followed by detection using polymer HRP Ms + Rb. FOXP3 was visualized using Opal 620 (1:100). The slides were again placed in citrate buffer (pH 6.0) and heated using a microwave. After the slides cooled, they were incubated with primary rabbit antibodies against IL-17A (NBP1-76337, 1:500; Novus Biologicals, Centennial, CO, USA) for 1 h in a humidified chamber at 4 °C followed by detection using polymer HRP Ms + Rb. IL-17A was visualized using Opal 690 (1:100). Lastly, the slides were again placed in citrate buffer (pH 6.0) and heated using a microwave. Nuclei were visualized with DAPI (1:500), and the sections were mounted using mounting media

(HIGHDEF® ADI-950-260-0025, Enzo Life Sciences, Farmingdale, NY, USA). The slides were incubated with rabbit antibodies against F4/80 (ab111101, 1:100; Abcam) as described above. For antigen retrieval, the slides were heated in citrate buffer (pH 9.0) using a microwave. The slides were then incubated with primary antibodies against F4/80 overnight in a humidified chamber at 4 °C. F4/80 was visualized using Opal 690 (1:100). The stained slides were scanned using SLIDEVIEW VS200 (Olympus, Tokyo, Japan). Data were analyzed using HALO v3.1.1076 (Indica Labs, Albuquerque, NM, USA).

Induction of arthritis and ankylosis in SKG mice

SKG mice were obtained from Dr. S. Sakaguchi[25]. Eight-week-old male SKG mice were intraperitoneally injected with either 3 mg of curdlan (FUJIFILM Wako Chemicals, Richmond, CA, USA) suspended in 0.2 mL of PBS (n = 34) or 0.2 mL PBS (n = 34) at 0 and 2 weeks. Control, non-model, 8-week-old male BALB/c mice were intraperitoneally injected with 0.2 mL of PBS at 0 and 2 weeks (n = 17). Clinical peripheral arthritis scores were measured every week for up to 21 weeks post-curdlan injection. All mice were maintained in a specific pathogen-free facility until whole-body images were obtained under a 12-hour light:dark cycle with free access to food and water. Mice were sacrificed at 23 weeks post-curdlan injection, and then splenocytes and the left hind region were collected. All animal experiments were performed in accordance with the guidelines for animal care approved by the

Animal Experimentation Committee of the Asan Institute for Life Sciences (2021-14-226).

Cigarette smoke exposure

One half of the curdlan-injected SKG mice (n = 17) and the PBS-injected SKG mice (n = 17) were exposed to smoke from 3R4F cigarettes (8.0 mg of tar/cigarette and 0.70 mg of nicotine/cigarette, Camel) as previously described, with some modifications [26]. The non-cigarette smoke-exposed group inhaled only room air. After gradual escalation to allow the mice to adapt to the smoke, they were exposed to cigarette smoke from four cigarettes for 15 min three times, with a 10 min rest in between. This was repeated three times, 5 days a week for 20 weeks starting with the first curdlan injection. Briefly, all mice were placed in an inhalation box (50 × 40 × 30 cm) connected to a pump and exposed to mainstream cigarette smoke simultaneously generated from four cigarettes for 15 minutes. Then, the box was ventilated to remove the cigarette smoke, and the mice breathed normal room air for 10 minutes. This process was repeated for two additional exposures.

Liquid chromatography-tandem mass spectrometry (LC-MS/MS)

Mouse serum was obtained at 16 weeks after the first curdlan injection. Collected blood was allowed to clot for a minimum of 1 h at room temperature and then centrifuged at 16,000 × g for 15 min at 4 °C. The separated mouse serum was

collected and stored at -80 °C until use. Cotinine standard and internal standards were purchased from Cayman Chemical (Ann Arbor, MI, USA). All solvents, including water, were purchased from J. T. Baker (Phillipsburg, NJ, USA). For the analysis, 5 μL of mouse serum was mixed with 500 μL of ethyl acetate and 50 μL of internal standard solution (1 μM Cotinine-d3). The mixture was sonicated at 40 kHz for 30 min at room temperature and then centrifuged at 13,000 rpm for 15 min at 4 °C. The supernatant was collected and dried using a vacuum centrifuge. The dried matter was stored at -20 °C and reconstituted with 50 μL of acetonitrile prior to LC-MS/MS analysis. Cotinine was determined using LC-MS/MS with an Agilent 1290 HPLC (Waldbronn, Germany) coupled to a QTRAP 5500 mass spectrometer (ABSciex, Toronto, Canada). Separation was achieved using a reverse-phase column (Pursuit5 C18, 150 × 2.1 mm) with mobile phase A (0.1% formic acid in H2O) and mobile phase B (0.1% formic acid in methanol) under isocratic conditions (90% B) at 300 μL/min for 10 min. The column temperature was maintained at 30 °C. Each sample (10 μL) was injected into the LC-MS/MS system and ionized with a turbo spray ionization source. Multiple reaction monitoring was performed in positive ion mode, and the extracted ion chromatogram corresponding to the specific transition of cotinine (m/z 177.2→80.0) was used for quantification. The calibration range for cotinine was 0.01–10 nM ($r2 \geq 0.99$). Data were analyzed using Analyst 1.7.1 software.

Clinical scoring of peripheral arthritis

The mice were monitored weekly for clinical features of peripheral arthritis and scored for severity on a scale of 0–4 (0 = no swelling, 1 = mild swelling and redness on the top of the foot, 2 = severe swelling and redness on the top of the foot, 3 = severe swelling and redness of the wrist or ankle joints, and 4 = severe swelling of the wrist or ankle joints and digits) [21]. The arthritic scores of the affected joints were combined to obtain a composite score for all paws.

Histological analysis

The excised left hind regions were fixed in 10% buffered formalin and then incubated in Calci-Clear Rapid (National Diagnostics, Atlanta, GA, USA) for 48 h for decalcification. Fixed tissues were rinsed with tap water to remove the formalin for about 2 h. Tissues were then dehydrated in graded ethanol and cleared with xylene using a tissue processor (Shandon Diagnostics, Excelsior AS) and embedded into paraffin using a paraffin embedding station (EG1150H; Leica, Wetzlar, Germany). The paraffin blocks were cut into 3 μm-thick sections on a rotary microtome (RM2255; Leica) and placed onto glass slides. Hematoxylin and eosin (H&E) staining and mounting with coverslips were performed using an automatic stainer (Leica autostainer, XL). Semiquantitative scoring of joint inflammation severity on a scale of 0–3 was performed in accordance with Standardized Microscopic Arthritis Scoring of Histological sections (SMASH) [27].

Surface and intracellular staining of splenocytes and flow cytometry analysis.

At 23 weeks after curdlan injection, the spleen was collected and filtered through a 100-μm nylon filter. Erythrocytes in the filtered cells were lysed using red blood cell lysis buffer (BioLegend, San Diego, CA, USA). The remaining cells were collected by centrifugation. Dead cells were excluded from the analysis using fixable viability dye (eFluor 506; eBioscience, CA, USA). Flow cytometry data were acquired using a FACS Canto II (BD Biosciences, CA, USA) and analyzed using Flow Jo software (Tree Star, OR, USA) as previously described [23]. Anti-mouse CD16/32 (BioLegend, clone: 93) was used to block Fc receptors, and surface markers were stained using the following antibodies: PerCP/Cy5.5-conjugated anti-CD4 (BioLegend, clone: GK1.5), APC/Cy7-conjugated anti-CD3 (BioLegend, clone: 17A2), and BV421-conjugated anti-CD25 (BioLegend, clone: PC61). After fixation and permeabilization, cytokines and transcription factors were stained with the following antibodies: PE-conjugated anti-RORγt (BD Biosciences, clone: Q31-378), PE/Cy7-IL-17A (BioLegend, clone: TC11-18H10.1), and Alexa Fluor 647-conjugated anti-FOXP3 (BioLegend, clone: 150D).

Imaging with fluorescent in vivo bisphosphonate agent

Whole-body imaging was performed at 21 weeks post-curdlan injection after depilation of the back using the fluorescent in vivo bisphosphonate agent OsteoSense® 680 EX (PerkinElmer, Waltham, MA, USA). Mice were injected with the bisphosphonate agent (2 nmol in 100 μL of PBS) via the tail vein. After 18 h,

fluorescent images were obtained using an IVIS spectrum system (Perkin Elmer) at excitation and emission wavelengths of 675 and 720 nm, respectively, under inhalation anesthesia. After acquisition, images were spectrally unmixed (Living Image software; Caliper Life Sciences, MA, USA). ROIs with the same area were placed and measured as the mean radiant efficiency.

Statistical analysis and Schematic diagram

All analyses were performed using GraphPad Prism 8.4.3 software (GraphPad Software, San Diego, CA, USA). Mann–Whitney U tests were performed for two-group comparisons. Results are presented as the mean ± standard error of the mean (SEM). P values less than 0.05 were considered statistically significant, and significant differences are indicated with asterisks as follows: *$p < 0.05$, **$p < 0.01$, ***$p < 0.001$, and ****$p < 0.0001$. All schematic diagrams were created at BioRender.com.

RESULTS

Expression of α7nAChRs, IL-17A, FOXP3 and F4/80 in the synovium of curdlan-administered SKG mice

Immunofluorescent staining was performed to confirm whether α7nAChR$^+$ cells were present in the synovial tissue of curdlan-administered SKG mice. Opal multiplexed immunofluorescent staining was performed on the left hind joint. The results showed that the α7nAChR$^+$ cells were increased in the joints of curdlan-administered SKG mice. IL-17A$^+$, FOXP3$^+$IL-17A$^+$, α7nAChR$^+$IL-17A$^+$, α7nAChR$^+$ IL-17A$^+$FOXP3$^+$, and α7nAChR$^+$F4/80$^+$ cells were also increased (Figure1).

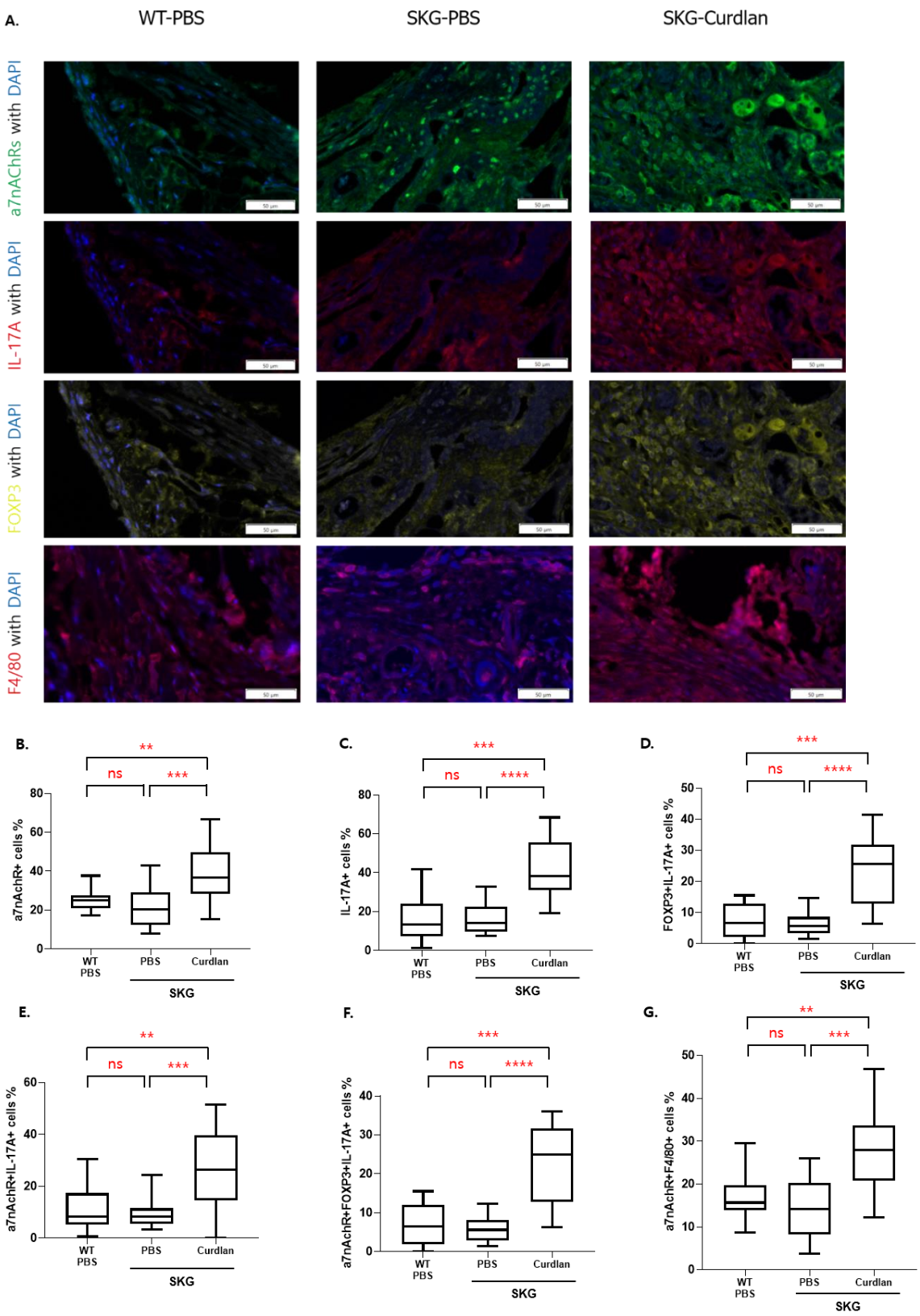
A.
WT-PBS
SKG-PBS
SKG-Curdlan
a7nAChRs with DAPI
IL-17A with DAPI
FOXP3 with DAPI
F4/80 with DAPI
B.
a7nAchR+ cells %
C.
IL-17A+ cells %
D.
FOXP3+IL-17A+ cells %
E.
a7nAchR+IL-17A+ cells %
F.
a7nAchR+FOXP3+IL-17A+ cells %
G.
a7nAchR+F4/80+ cells %
ns
**
***
****
WT
PBS
PBS
Curdlan
SKG

Figure 1. Opal multiplexed immunofluorescent images and semi-quantitation. (A) Opal multiplexed immunofluorescent images that show the α7nAChRs^{+} cells, IL-17A^{+} cells, FOXP3^{+} cells and F4/80^{+} cells in the hind tissue. (B) α7nAChRs^{+} cells. (C) IL-17A^{+} cells. (D) FOXP3^{+}IL17A^{+} cells. (E) α7nAChRs^{+} IL17A^{+} cells. (F) α7nAChRs^{+}FOXP3^{+}IL17A^{+} cells. (G) α7nAChRs^{+}F4/80^{+} cells. Immunization using curdlan affects immune cell population in the hind of SKG mice. *$p \leq 0.05$, ***$p \leq 0.001$, ****$p \leq 0.0001$.

Experimental design

A mouse model was used to investigate the role of α7nAChR activation by nicotine and cotinine from cigarette smoke on arthritis and spinal ankylosis in SpA. The experimental design is shown in Figure 2. SKG mice were injected with curdlan at 0 and 2 weeks to establish the SpA model. SKG mice and BALB/c mice intraperitoneally injected with PBS alone at 0 and 2 weeks were used as controls. In the cigarette smoke-exposed group, after gradual escalation to adapt the mice to the smoke, they were exposed to smoke from four cigarettes for 15 min three times with 10 min rest 5 days a week for 20 weeks starting with the first curdlan injection.

Figure 2. Experimental design, survival proportions and the clinical score of peripheral arthritis

Experimental design. 8-week-old male SKG mice were intraperitoneally injected with 3 mg curdlan at 0 and 2 weeks. Gradually adjust to cigarette smoke a week before the curdlan injection. The cigarette smoking exposure was performed for 20 weeks post curdlan injection. At 16 weeks post curdlan injection, the mice blood collected and fluorescence imaging of HA was performed at 20 weeks post curdlan injection. Then, at 23 weeks post curdlan injection, all mice were sacrificed.

Metabolomic analysis of cotinine levels

We conducted a metabolic analysis of mouse serum obtained 16 weeks after the first curdlan injection to determine which of the metabolites in cigarettes are dominant. Nicotine was not detected (data not shown); however, cotinine was significantly increased in cigarette smoke-exposed curdlan-administered SKG mice compared with that in the unexposed mice (Figure 3). Cotinine is used as a biomarker for cigarette smoking because of its long half-life [28]. These results suggested that the smoking model was sufficient, and nicotine was metabolized to cotinine, which had an effect on SKG mice.

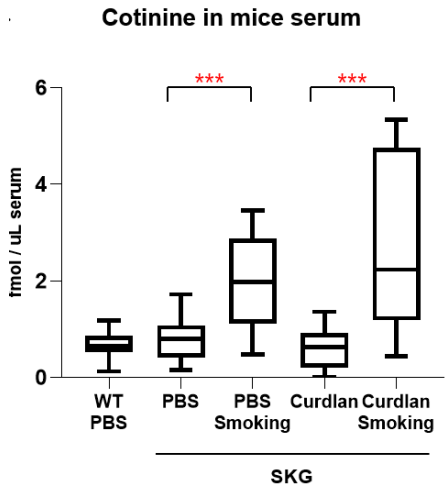

Figure 3. Smoking metabolites in serum of mice. (A) cotinine level of mice serum. In all groups exposed to cigarette smoke, the concentration of cotinine was higher than in the group not exposed to cigarette smoke. ***$p \leq 0.001$

Effects of cigarette smoke on peripheral arthritis

Mice were examined weekly for clinical signs of arthritis in peripheral joints. From 5 weeks after curdlan administration, the peripheral arthritis score was significantly lower in cigarette smokie-exposed curdlan-administered SKG mice than in unexposed mice (Figure 4A). However, this difference was not observed after 16 weeks post curdlan administration because half of the mice exposed to cigarette smokie died (Figure 4B).

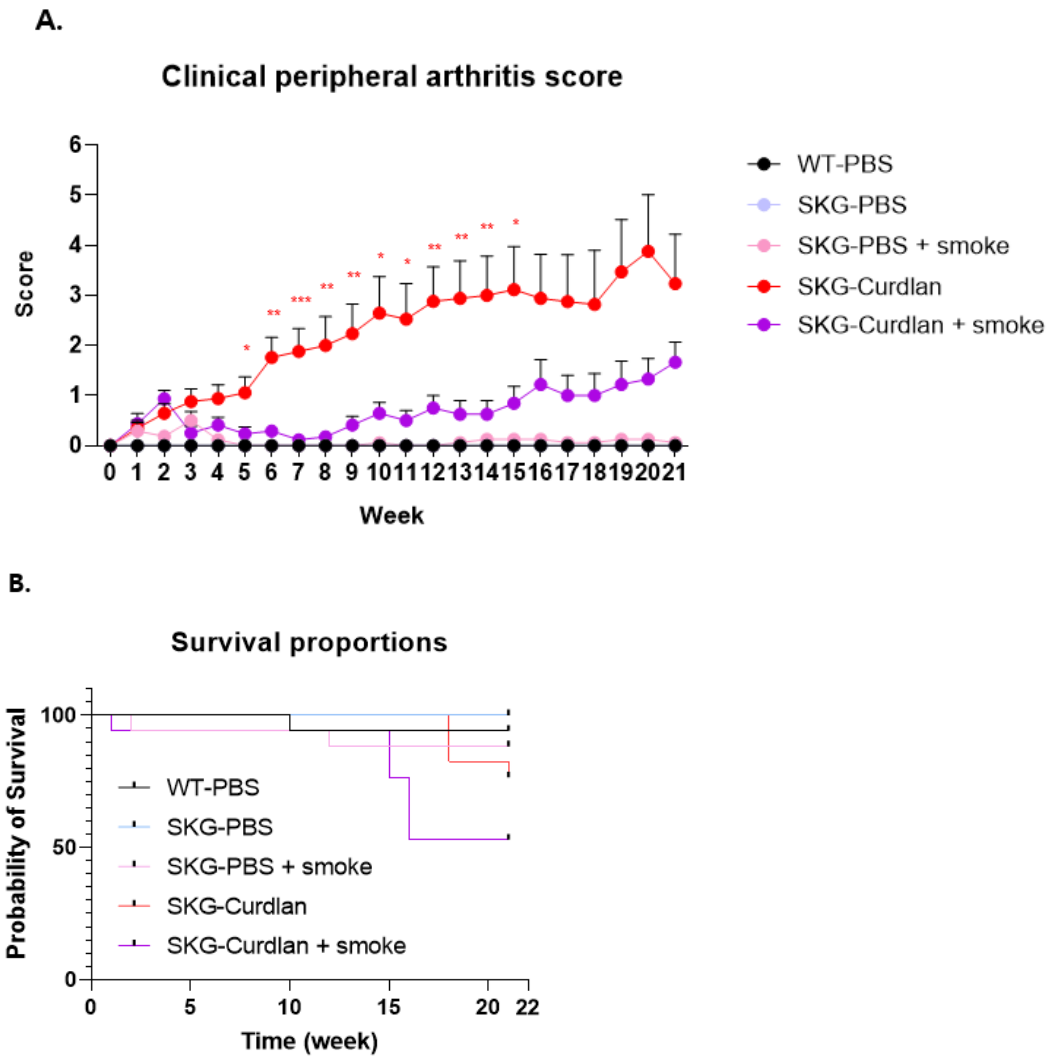

Figure 4. Survival proportions and the clinical score of peripheral arthritis

(A) Clinical peripheral arthritis score. The arthritis scores were examined every week for up to 21 weeks after curdlan injection. (B) Survival proportions. At 15 weeks post curdlan injection, the population of curdlan-administered SKG mice with cigarette smoke has halved. *$p \leq 0.05$, **$p \leq 0.01$, ***$p \leq 0.001$ between curdlan-administered SKG mice with smoking and those without smoking.

Histologic examination in the peripheral joint

For the histological examination, the left hind region of the mice was stained with H&E. An anatomical schematic diagram of the hind region and representative magnified images of all groups are shown in Figure 5A. H&E staining can reveal joint inflammation, inflammatory cell infiltration, and the thickening and increase of synoviocytes [27]. Unexposed curdlan-administered SKG mice had the most severe arthritis. Semiquantitative scores of joint inflammation also showed the most severe arthritis in unexposed curdlan-administered SKG mice. There was no difference between PBS-administered SKG mice and cigarette smoke-exposed curdlan-administered SKG mice (Figure 5B).

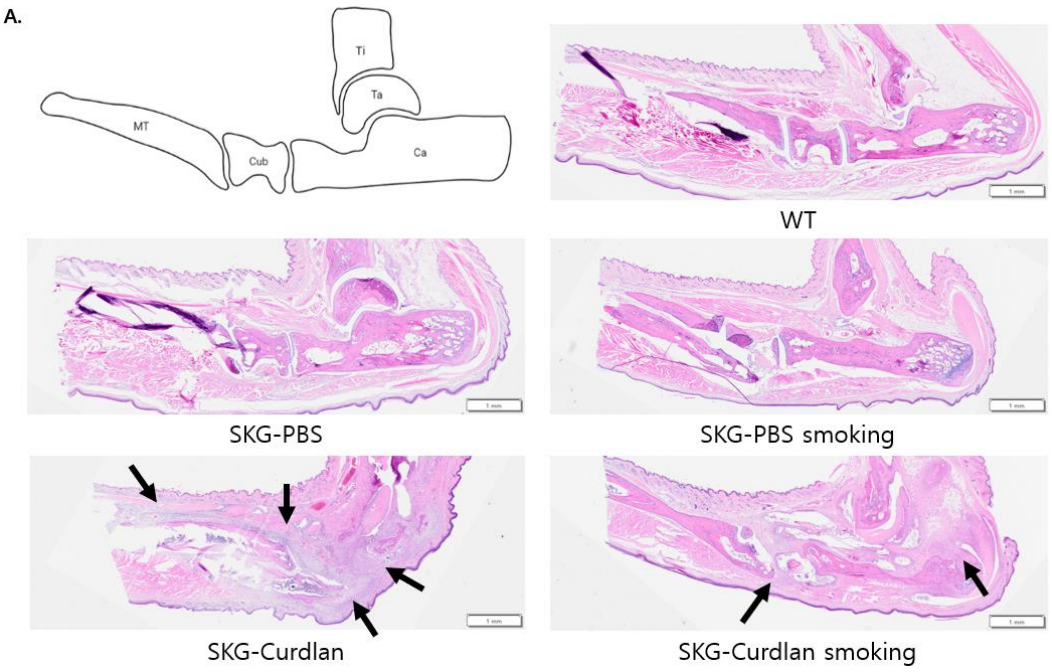

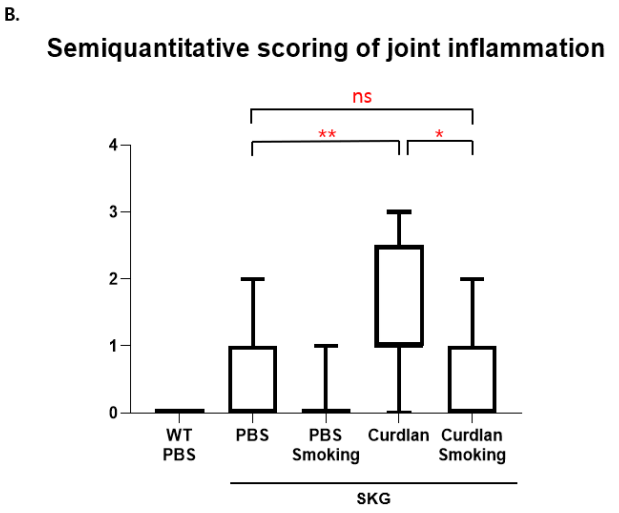

Figure 5. Histologic examination of the hind from SKG mice at 22 weeks after a curdlan injection with/without cigarette smoking. (A) The representative magnified images of H&E staining of all groups. Original magnification is 200x. (B) Semiquantitative scoring of joint inflammation. Curdlan-administered SKG mice without cigarette smoke have bandy leg and most severe inflammation.

Curdlan-administered SKG mice with cigarette smoke also have inflammation, but it is less severe. The arrows indicate the inflammatory infiltrated cells. Ca, calcaneus; Cub, cuboid; MT, metatarsal; Ta, talus; Ti, tibia. *$p \leq 0.05$, **$p \leq 0.01$.

Alteration of T cell population in the splenocytes

IL-17A-expressing cells play an important role of the pathogenesis in SpA [22, 24, 29]. We conducted a flow cytometry analysis of spleen cells. We investigated the characteristics of the T cell populations in the spleens of mice using anti-CD3, CD4, CD25, FOXP3, IL-17A, and RORγt antibodies (Figure 6A). The T_H17 cell and regulatory T (T_{reg}) cell populations did not differ between the cigarette smoke-exposed and unexposed curdlan-administered SKG mice (Figure 6B, 6C); however, the IL-17A$^+$ T_{reg} population was decreased in the cigarette smoke-exposed group.

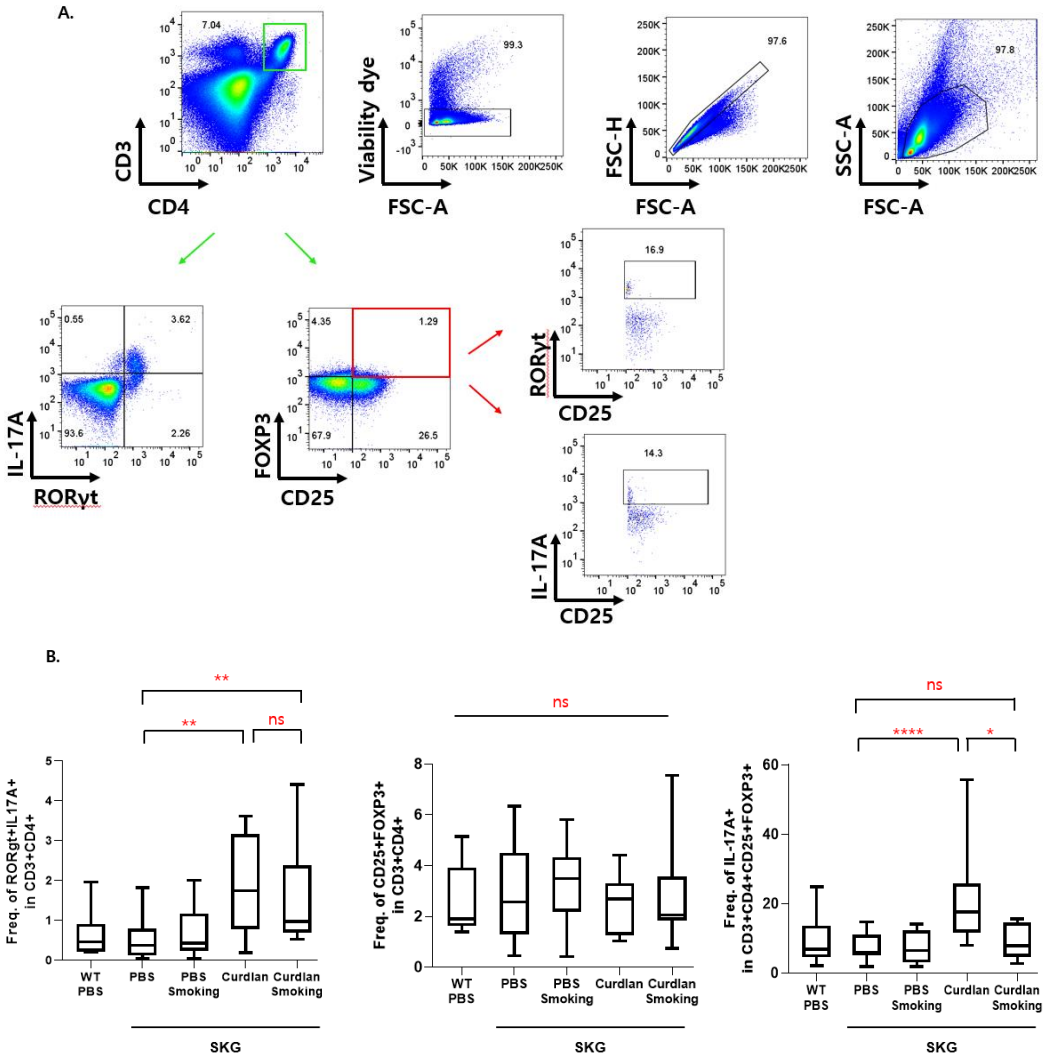

Figure 6. Flow cytometry of splenocyte in the mice. (A) Flow cytometry strategy. (B) Proportion of T_H17 (IL-17A$^+$RORγt$^+$ in CD3$^+$CD4$^+$ cells), T_{reg} (CD25$^+$FOXP3$^+$ in CD3$^+$CD4$^+$ cells), IL-17A$^+$ T_{reg} (IL-17A$^+$FOXP3$^+$CD25$^+$ in CD3$^+$CD4$^+$ cells). *p ≤ 0.05, **p ≤ 0.01, ****p ≤ 0.0001.

Osteoblast activity in the spine

The mice were evaluated for osteoblast activity by evaluating the accumulation of hydroxyapatite using a fluorescent in vivo bisphosphonate imaging agent (OsteoSense 680 EX). A representative biodistribution of fluorescence signals on the mouse spine is shown in Figure 7A. Curdlan-administered SKG mice had higher fluorescence signals than in PBS-administered SKG mice; however, cigarette smoke exposure did not alter osteoblast activity in curdlan-administered SKG mice (Figure 7B).

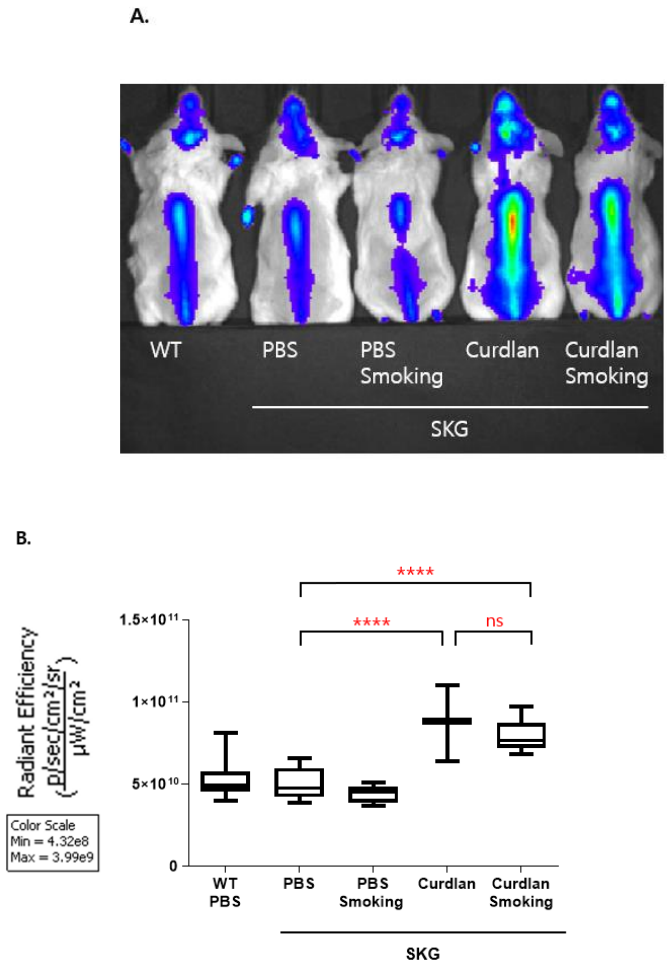

Figure 7. Imaging with fluorescent in vivo bisphosphonate agent.

(A) Fluorescence imaging of hydroxyapatite (HA) at spine and (B) quantitative analysis of fluorescence values. Curdlan-administered SKG mice had high fluorescence signals, however, no difference was found between the mice with cigarette smoke or not. ****$p \leq 0.0001$

Discussion

Curdlan-administered SKG mice had increased numbers of α7nAChR$^+$ and IL-17A$^+$ cells and higher clinical arthritis scores at peripheral joints. However, the clinical arthritis score and histologic inflammation were improved in cigarette smoke-exposed curdlan-administered SKG mice, suggesting that a component of cigarette smoke, cotinine, a major metabolite of nicotine, may inhibit inflammation in curdlan-administered SKG mice. Unlike nicotine, cotinine has no withdrawal effects, and it is safe to administer 10 times as much as cotinine as that detected in a typical human smoker for a short period of time [30]. Therefore, cotinine might be a suitable compound for improving SpA.

The cholinergic anti-inflammatory pathway involves the interaction between the autonomic nervous system and the immune system, and the neurotransmitter acetylcholine and its receptors, particularly alpha 7 subunit nicotinic acetylcholine receptor, α7nAChR, play an important role [31]. α7nAChR is expressed in a variety of immune cells, including dendritic cells, T and B lymphocytes, monocytes, and macrophages [7]. Nicotine, as well as its metabolite cotinine, can activate α7nAChR [32], In our metabolomic analysis, nicotine was not detected because of its very short half-life. Although α7nAChR is mainly expressed on macrophages and fibroblasts in synovial tissues from patients with RA and psoriatic arthritis [33], there are few studies on the relationship between α7nAChR and SpA. Here, we reported that α7nAChR was highly expressed in immune cells residing in the synovia of curdlan-administered SKG mice.

In SpA, excessive new bone formation occurs in response to mechanical stress, and disease pathogenesis is related to the interaction between inflammatory cells and bone cells [34]. Unlike in a SpA cohort study suggesting that smoking caused structural damage to the spine and cigarette smoke induced oxidative stress by increasing superoxide radicals, which negatively affected osteogenic differentiation, nicotine and cotinine did not directly affect osteogenic differentiation but negatively affected the osteogenic differentiation of mesenchymal stem cells [35]. We observed a decrease in IL-17A$^+$ cells in the synovia, suggesting that IL-17A levels were also decreased in the model mice. IL-17A induces enthesitis by promoting osteoclast formation, but its effect on osteoblast differentiation may vary depending on the cell type, the differentiation stage of the cell, and the timing and duration of exposure [36]. In our study, cigarette smoke did not alter the osteogenic activity in the model mice (Figure 7). Osteogenic activity and bone formation might be affected by oxidative stress induced by cigarette smoke and the levels of inflammatory cytokines such as IL-17.

Cigarette smoke is a mixture of numerous chemicals that can directly or indirectly affect the immune system [37]. Cigarette smoking is a poor prognostic factor for RA and AS, which are related to autoimmune inflammation [38, 39]. However, cigarette smoke reduced anti-cyclic citrullinated peptides and slowed the onset and progression of arthritis in CIA mice [40]. A few studies have examined the relationship between cigarette smoking and symptoms of SpA. In a Norwegian population case-control study, smokers were twice as likely to self-report AS as

non-smokers [41]. However, the cohort was atypical, with more females than males, and the independent causal relationship of smoking is uncertain [42]. In an early axial SpA cohort, smoking was independently associated with earlier onset of inflammatory back pain and increasing axial inflammation [43]. Other studies have shown a correlation between back pain or disease activity and smoking but no correlation between smoking and the onset of symptoms In all five studies, smoking was found to advance the onset of symptoms by an average of 0.1 years, and there was no statistically or clinically significant difference between current smokers and non-smokers [42]. Although there have been several studies on the link between habitual smoking and axial SpA [39, 43-46], the evidence supporting the independent role of smoking in disease onset is not consistent [42]. Further, no study using an experimental animal model has found an effect of cigarette smoke, and no study has found an effect of nicotine or cotinine on SpA. Thus, this study is meaningful as it is the first animal study to find a relationship between cigarette smoke and SpA phenotypes.

In our study, the fatality rate of cigarette smoke-exposed curdlan-administered SKG mice was almost 50% (Figure 4B). Cigarette smoking is generally harmful, and continuous smoking can cause serious lung and cardiovascular diseases [47] and increase the risk of cancer [48]. However, cigarette smoke contains a mixture of thousands of chemicals, each of which can have both beneficial and harmful direct or indirect effects on the immune system [37].

Nicotine has been shown to have both inflammatory and anti-inflammatory effects. Nicotine suppresses the immunity by acting on neutrophils, antigen-presenting cells, and macrophages and inhibiting inflammatory cytokines [13]. Nicotine also has pro-inflammatory effects, including promoting the T_H2 pathway and increasing the levels of pro-inflammatory cytokines and free radicals [37]. In Lewis rats, administration of nicotine before immunization aggravated arthritis, whereas administration of nicotine after immunization suppressed arthritis [49]. Our mouse model was exposed to cigarette smoke at the time of curdlan administration, but it suppressed arthritis. This may be owing to differences in the phenotype and pathogenesis of the animal models used.

Cotinine is a minor alkaloid of cigarettes [50] and major a metabolite of nicotine, the predominant alkaloid in cigarettes [16, 17]. Like nicotine, cotinine is an agonist of α7nAChR [51], and it also is attracting attention as a neuropharmacological agent. The neuropharmacological effects of nicotine are difficult to explain pharmacologically, given its short half-life. However, its effects may be due to cotinine, which elicits a similar pharmacological response as nicotine, and has a longer half-life [52]. In other words, it suggests that the continuous effect through cotinine can be seen compared to nicotine in the inflammatory reaction via α7nAChR.

IL-17, which is mainly produced by T_H17 cells, plays an important role in inflammatory diseases [53]. T_H17 cells were much more frequent among the peripheral blood monocyte cells of patients with AS than in healthy controls [54].

Serum IL-17 levels were also higher in patients with AS than in healthy controls [55]. In this study, cigarette smoke decreased the proportions of IL-17A$^+$, IL-17A$^+$FOXP3$^+$, and α7nAChR$^+$IL-17A$^+$FOXP3$^+$ cells in the hind region of curdlan-administered SKG mice, resulting in an anti-arthritogenic reaction. IL-17A levels may be reduced through a mechanism that inhibits the nuclear factor-kappa binding (NFκB) or Janus kinase/signal transduction and activator of transcription (JAK-STAT) signaling pathway through receptor activation [31].

The present study has several limitations. First, the metabolic and histologic analyses were performed at different time points. However, we thought that cotinine levels would not change during continuous smoking. Second, there is no in vitro experiment that can reveal the mechanism underlying the association between cotinine and peripheral arthritis. These limitations should be considered in future studies.

In conclusion, our results are the first to suggest that cigarette smoke might ameliorate peripheral arthritis but not spinal mineralization with a concomitant increase in serum cotinine in curdlan-administered SKG model mice. Future in vivo and in vitro experiments using cotinine are needed to confirm the direct effect of cotinine on SpA phenotypes.

REFERENCE

1. van der Heijde, D., et al., *2016 update of the ASAS-EULAR management recommendations for axial spondyloarthritis.* Ann Rheum Dis, 2017. **76**(6): p. 978-991.
2. Sieper, J., et al., *Axial spondyloarthritis.* Nature Reviews Disease Primers, 2015. **1**(1): p. 15013.
3. Gaston, J.S.H. and D.R. Jadon, *Th17 cell responses in spondyloarthritis.* Best Pract Res Clin Rheumatol, 2017. **31**(6): p. 777-796.
4. Ranganathan, V., et al., *Pathogenesis of ankylosing spondylitis - recent advances and future directions.* Nat Rev Rheumatol, 2017. **13**(6): p. 359-367.
5. Komatsu, N., et al., *Pathogenic conversion of Foxp3+ T cells into TH17 cells in autoimmune arthritis.* Nat Med, 2014. **20**(1): p. 62-8.
6. Li, Z., et al., *FOXP3+ regulatory T cells and their functional regulation.* Cellular & Molecular Immunology, 2015. **12**(5): p. 558-565.
7. Lv, J., et al., *The role of the cholinergic anti-inflammatory pathway in autoimmune rheumatic diseases.* Scandinavian Journal of Immunology, 2021. **94**(4): p. e13092.
8. Maanen, M.A.V., et al., *The α7 nicotinic acetylcholine receptor on fibroblast-like synoviocytes and in synovial tissue from rheumatoid arthritis patients: A possible role for a key neurotransmitter in synovial inflammation.* Arthritis & Rheumatism, 2009. **60**(5): p. 1272-1281.
9. van Maanen, M.A., et al., *Two novel alpha7 nicotinic acetylcholine receptor ligands: in vitro properties and their efficacy in collagen-induced arthritis in mice.* PLoS One, 2015. **10**(1): p. e0116227.
10. Liu, Z., et al., *Activation of α7nAChR by Nicotine Reduced the Th17 Response in CD4+T Lymphocytes.* Immunological Investigations, 2014. **43**(7): p. 667-674.
11. Wang, D.W., et al., *Stimulation of alpha7 nicotinic acetylcholine receptor by nicotine increases suppressive capacity of naturally occurring CD4+CD25+ regulatory T cells in mice in vitro.* J Pharmacol Exp Ther, 2010. **335**(3): p. 553-61.
12. Han, X., et al., *Stimulation of α7 Nicotinic Acetylcholine Receptor by Nicotine Suppresses Decidual M1 Macrophage Polarization Against Inflammation in Lipopolysaccharide-Induced Preeclampsia-Like Mouse Model.* Frontiers in Immunology, 2021. **12**.
13. Zhang, W., et al., *Nicotine in Inflammatory Diseases: Anti-Inflammatory and Pro-*

Inflammatory Effects. Front Immunol, 2022. **13**: p. 826889.

14. Yang, Y., et al., *Regulatory effect of nicotine on collagen-induced arthritis and on the induction and function of in vitro-cultured Th17 cells.* Modern Rheumatology, 2014. **24**(5): p. 781-787.
15. Li, S., et al., *Activation of the cholinergic anti-inflammatory system by nicotine attenuates arthritis via suppression of macrophage migration.* Mol Med Rep, 2016. **14**(6): p. 5057-5064.
16. Benowitz, N.L. and P. Jacob III, *Metabolism of nicotine to cotinine studied by a dual stable isotope method.* Clinical Pharmacology & Therapeutics, 1994. **56**(5): p. 483-493.
17. Zhu, A.Z., et al., *The ability of plasma cotinine to predict nicotine and carcinogen exposure is altered by differences in CYP2A6: the influence of genetics, race, and sex.* Cancer Epidemiol Biomarkers Prev, 2013. **22**(4): p. 708-18.
18. Rehani, K., et al., *Cotinine-induced convergence of the cholinergic and PI3 kinase-dependent anti-inflammatory pathways in innate immune cells.* Biochim Biophys Acta, 2008. **1783**(3): p. 375-82.
19. Barreto, G.E., A. Iarkov, and V.E. Moran, *Beneficial effects of nicotine, cotinine and its metabolites as potential agents for Parkinson's disease.* Frontiers in Aging Neuroscience, 2015. **6**.
20. Bessis, N., et al., *Arthritis models: usefulness and interpretation.* Semin Immunopathol, 2017. **39**(4): p. 469-486.
21. Ruutu, M., et al., *β-glucan triggers spondylarthritis and Crohn's disease–like ileitis in SKG mice.* Arthritis & Rheumatism, 2012. **64**(7): p. 2211-2222.
22. Rahman, M.A. and R. Thomas, *The SKG model of spondyloarthritis.* Best Practice & Research Clinical Rheumatology, 2017. **31**(6): p. 895-909.
23. Lim, D.-H., et al., *Effect of tumor necrosis factor inhibition on spinal inflammation and spinal ankylosis in SKG mice.* Scientific Reports, 2019. **9**(1): p. 18000.
24. Benham, H., et al., *Interleukin-23 Mediates the Intestinal Response to Microbial β-1,3-Glucan and the Development of Spondyloarthritis Pathology in SKG Mice.* Arthritis & Rheumatology, 2014. **66**(7): p. 1755-1767.
25. Hirota, K., et al., *Autoimmune Th17 Cells Induced Synovial Stromal and Innate Lymphoid Cell Secretion of the Cytokine GM-CSF to Initiate and Augment Autoimmune Arthritis.* Immunity, 2018. **48**(6): p. 1220-1232.e5.
26. Jang, Y.O., et al., *Fecal microbial transplantation and a high fiber diet attenuates emphysema development by suppressing inflammation and apoptosis.* Exp Mol Med, 2020. **52**(7): p. 1128-1139.

27. Hayer, S., et al., *'SMASH' recommendations for standardised microscopic arthritis scoring of histological sections from inflammatory arthritis animal models.* Ann Rheum Dis, 2021.
28. Hukkanen, J., P. Jacob, 3rd, and N.L. Benowitz, *Metabolism and disposition kinetics of nicotine.* Pharmacol Rev, 2005. **57**(1): p. 79-115.
29. Jeong, H., et al., *Spondyloarthritis features in zymosan-induced SKG mice.* Joint Bone Spine, 2018. **85**(5): p. 583-591.
30. Hatsukami, D.K., et al., *Safety of Cotinine in Humans: Physiologic, Subjective, and Cognitive Effects.* Pharmacology Biochemistry and Behavior, 1997. **57**(4): p. 643-650.
31. van Maanen, M.A., M.J. Vervoordeldonk, and P.P. Tak, *The cholinergic anti-inflammatory pathway: towards innovative treatment of rheumatoid arthritis.* Nature Reviews Rheumatology, 2009. **5**(4): p. 229-232.
32. Martin, L.F., W.R. Kem, and R. Freedman, *Alpha-7 nicotinic receptor agonists: potential new candidates for the treatment of schizophrenia.* Psychopharmacology, 2004. **174**(1): p. 54-64.
33. Westman, M., et al., *Cell Specific Synovial Expression of Nicotinic Alpha 7 Acetylcholine Receptor in Rheumatoid Arthritis and Psoriatic Arthritis.* Scandinavian Journal of Immunology, 2009. **70**(2): p. 136-140.
34. Nakamura, A., et al., *Bone formation in axial spondyloarthritis: Is disease modification possible?* Best Practice & Research Clinical Rheumatology, 2019. **33**(6): p. 101491.
35. Aspera-Werz, R.H., et al., *Nicotine and Cotinine Inhibit Catalase and Glutathione Reductase Activity Contributing to the Impaired Osteogenesis of SCP-1 Cells Exposed to Cigarette Smoke.* Oxidative medicine and cellular longevity, 2018. **2018**: p. 3172480-3172480.
36. Gravallese, E.M. and G. Schett, *Effects of the IL-23-IL-17 pathway on bone in spondyloarthritis.* Nat Rev Rheumatol, 2018. **14**(11): p. 631-640.
37. Arnson, Y., Y. Shoenfeld, and H. Amital, *Effects of tobacco smoke on immunity, inflammation and autoimmunity.* Journal of Autoimmunity, 2010. **34**(3): p. J258-J265.
38. Ishikawa, Y. and C. Terao, *The Impact of Cigarette Smoking on Risk of Rheumatoid Arthritis: A Narrative Review.* Cells, 2020. **9**(2).
39. Zhao, S., et al., *Associations between smoking and extra-axial manifestations and disease severity in axial spondyloarthritis: results from the BSR Biologics Register for Ankylosing Spondylitis (BSRBR-AS).* Rheumatology (Oxford), 2019.

58(5): p. 811-819.

40. Lindblad, S.S., et al., *Smoking and nicotine exposure delay development of collagen-induced arthritis in mice.* Arthritis Res Ther, 2009. **11**(3): p. R88.
41. Videm, V., et al., *Current Smoking is Associated with Incident Ankylosing Spondylitis — The HUNT Population-based Norwegian Health Study.* The Journal of Rheumatology, 2014. **41**(10): p. 2041-2048.
42. Zhao, S.S., et al., *Smoking in spondyloarthritis: unravelling the complexities.* Rheumatology (Oxford), 2020. **59**(7): p. 1472-1481.
43. Chung, H.Y., et al., *Smokers in early axial spondyloarthritis have earlier disease onset, more disease activity, inflammation and damage, and poorer function and health-related quality of life: results from the DESIR cohort.* Annals of the Rheumatic Diseases, 2012. **71**(6): p. 809-816.
44. Chen, C.-H., et al., *Association of cigarette smoking with Chinese ankylosing spondylitis patients in Taiwan: a poor disease outcome in systemic inflammation, functional ability, and physical mobility.* Clinical Rheumatology, 2013. **32**(5): p. 659-663.
45. Zhang, H., et al., *Smoking quantity determines disease activity and function in Chinese patients with ankylosing spondylitis.* Clinical Rheumatology, 2018. **37**(6): p. 1605-1616.
46. Zhao, S., et al., *Increasing smoking intensity is associated with increased disease activity in axial spondyloarthritis.* Rheumatology International, 2017. **37**(2): p. 239-244.
47. Ambrose, J.A. and R.S. Barua, *The pathophysiology of cigarette smoking and cardiovascular disease: An update.* Journal of the American College of Cardiology, 2004. **43**(10): p. 1731-1737.
48. Jassem, E., et al., *Smoking and lung cancer.* Advances in Respiratory Medicine, 2009. **77**(5): p. 469-473.
49. Yu, H., et al., *Nicotine-induced differential modulation of autoimmune arthritis in the Lewis rat involves changes in interleukin-17 and anti-cyclic citrullinated peptide antibodies.* Arthritis and rheumatism, 2011. **63**(4): p. 981-991.
50. Benowttz, N.L., et al., *Smokers of Low-Yield Cigarettes Do Not Consume Less Nicotine.* New England Journal of Medicine, 1983. **309**(3): p. 139-142.
51. Tan, X., K. Vrana, and Z.M. Ding, *Cotinine: Pharmacologically Active Metabolite of Nicotine and Neural Mechanisms for Its Actions.* Front Behav Neurosci, 2021. **15**: p. 758252.
52. Buccafusco, J.J. and A.V. Terry, *The potential role of cotinine in the cognitive and*

neuroprotective actions of nicotine. Life Sciences, 2003. **72**(26): p. 2931-2942.

53. Miossec, P., *IL-17 and Th17 cells in human inflammatory diseases.* Microbes and Infection, 2009. **11**(5): p. 625-630.
54. Shen, H., J.C. Goodall, and J.S. Hill Gaston, *Frequency and phenotype of peripheral blood Th17 cells in ankylosing spondylitis and rheumatoid arthritis.* Arthritis Rheum, 2009. **60**(6): p. 1647-56.
55. Mei, Y., et al., *Increased serum IL-17 and IL-23 in the patient with ankylosing spondylitis.* Clin Rheumatol, 2011. **30**(2): p. 269-73.

국문요약

콜린성 항염증 경로는 자율신경계와 면역계 사이의 상호작용으로 알려져 있는데, 특히 다양한 면역세포와 활막세포에서 발현되는 아세틸콜린 수용체의 구성원인 α7nAChRs이 주요한 역할은 한다. α7nAChR은 염증성 사이토카인의 분비를 억제하여 항염증 경로에서 중요한 역할을 한다. 니코틴의 주요 대사산물인 니코틴과 코티닌이 면역세포에서 α7nAChR을 활성화시켜 자가면역관절염에 항염증성을 가지고 있다는 연구가 많이 있다. 류마티스 관절염 환자의 활막에서 코티닌 수용체인 α7nAChRs의 발현이 증가하였다. 그러나 척추관절염에서의 α7nAChR의 역할에 대해서는 거의 알려져 있지 않다. 따라서 우리는 척추관절염의 모델인 커드란 투여 SKG 마우스에서 α7nAChR의 활막에서의 발현과 흡연을 이용하여 활성화시켜서 말초 관절염 및 척추관절증에 미치는 영향을 평가했다. 커드란을 2주 간격으로 2회 SKG 마우스에 복강투여하였고, 첫 번째 커드란 주사 이후 20주 동안 주 5일 (15분당 담배 4개비, 10분 반복 휴식) 담배 연기에 노출시키거나 노출시키지 않은 그룹으로 분리하였다. 혈청 코티닌의 대사 분석은 커드란 주사 후 16주에 수행하였다. 말초관절염에 대한 임상 점수는 매주 시행하였으며, 23주에 희생하여 조직학적 평가를 수행하였다. 척추의 골아세포 활성의 존재를 식별하기 위해 커드란 투여 후 21주째 형광물질 OsteoSense® 680 EX를 사용하여 영상을 촬영하였다. Flow cytometry를 통해 비장세포의 T 세포의 분포를

연구하였고, 왼쪽 뒷다리에서 면역조직화학적 염색을 시행하였다. 커드란 투여 후 23주 투여 시, 커드란 투여 SKG 마우스 활막에서 α7nAChRs$^+$ 및 α7nAChRs$^+$$T_H$17 세포가 증가하였다. 16주간의 커드란 주사 후 대사분석 결과 담배연기에 노출된 마우스에서 코티닌 수치가 증가하였다. 말초관절염 점수는 흡연을 하지 않은 SKG 마우스에서 더 높았다. 이러한 결과와 마찬가지로, 조직학적 검사에서도 흡연을 하지 않은 SKG 마우스에서 염증반응이 많이 나타났다. 그러나 척추의 골아세포 활성의 정도는 측정된 그룹 간에 차이가 없었다. Flow cytometry 분석에서 T_H17과 T_{reg}는 그룹 간 비율의 차이가 없었으나, 흡연을 하지 않고 커드란 투여한 SKG 마우스에서 IL-17A$^+$ T_{reg} 인구가 증가하였다. 또한 IL-17A$^+$ 세포, FOXP3$^+$ 세포 및 IL-17A$^+$FOXP3$^+$ 세포의 비율은 흡연을 하지 않은 는 SKG 생쥐의 활막에서 증가하였다.

우리의 연구 결과는 자가면역관절염 모델인 SKG 마우스의 활막에는 α7nAChRs$^+$ 세포가 많이 존재하며, 흡연을 통한 코티닌 증가를 통해 관절염에 치료 효과를 가질 수 있음을 시사한다.